

# Power dependent switching of nonlinear trapping by local photonic potentials

Y. Shavit,<sup>1</sup> Y. Linzon,<sup>1,\*</sup> S. Bar-Ad,<sup>1</sup> R. Morandotti,<sup>2</sup> M. Volatier-Ravat,<sup>3</sup> V. Aimez,<sup>3</sup> and R. Ares<sup>3</sup>

<sup>1</sup>*School of Physics and Astronomy, Faculty of Exact Sciences,  
Tel-Aviv University, Tel Aviv 69978, Israel*

<sup>2</sup>*Universite' du Quebec, Institute National de la Recherche  
Scientifique, Varennes, Quebec J3X 1S2, Canada*

<sup>3</sup>*Centre de Recherche en Nanofabrication et en Nanocaracterisation,  
Universite de Sherbrooke, Sherbrooke, J1K2R1, Canada*

*\*Corresponding author: linzonyo@post.tau.ac.il*

We study experimentally and numerically the nonlinear scattering of wave packets by local multi-site guiding centers embedded in a continuous dielectric medium, as a function of the input power and angle of incidence. The extent of trapping into the linear modes of different sites is manipulated as a function of both the input power and incidence angle, demonstrating power-controlled switching of nonlinear trapping by local photonic potentials. © 2019 Optical Society of America

*OCIS codes:* 190.4420, 290.0290, 230.7390.

Nonlinear two-dimensional (2D) wave scattering by local potential discontinuities has been the subject of extensive theoretical studies [1-9], and was recently realized experimentally

[10]. In the optical realization of 2D wave packet scattering in planar waveguides [10], photonic scattering centers are formed by local modulations of the refractive index, embedded in an otherwise homogeneous single-mode planar dielectric waveguide [see Figs. 1(a) and 1(b)]. Such centers, or "defects", can be either anti-guiding or guiding, with the latter type supporting internal normal modes. The normal modes can be excited by direct-excitation [Fig. 1(a)]. Radiation modes, coupled via side-excitation at an angle of incidence  $\theta$  towards the center [Fig. 1(b)], scatter from the local structure. In the linear-wave regime, the propagation of normal modes and the scattering of radiation modes are fully characterized by the structure's plane wave transmission spectrum [Figs. 1(c) and 1(d)]; Normal modes and linear radiation modes are also decoupled, so that energy conservation of the scattered transmitted and reflected wave packets is fulfilled:  $R + T = 1$ .

In the presence of a focusing Kerr nonlinearity, the scattering dynamics can change dramatically. In particular, the nonlinearity can couple light between the radiation modes and normal modes through the nonlinearity-induced change of the propagation constant [10], provided that the local modulations are shallow and a near-grazing angle of incidence (small

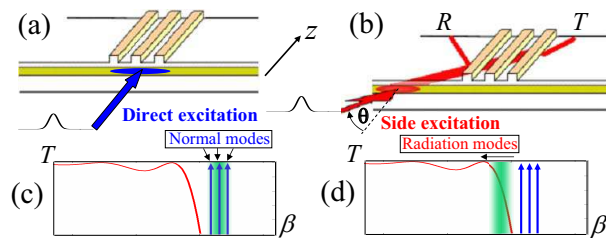


Fig. 1. (Color online) (a) Directly-excited normal modes of a local photonic structure, and (b) side-excited radiation modes scattering from this structure; (c), (d) a characteristic plane wave transmission spectrum. In the linear regime direct-excitations couple to normal modes (c), while side-excitations couple to radiation modes (d), each of which exist in different propagation constant ( $\beta$ ) regimes. Shaded regions in (c) and (d) indicate spatial frequency bands of corresponding input wave packets.

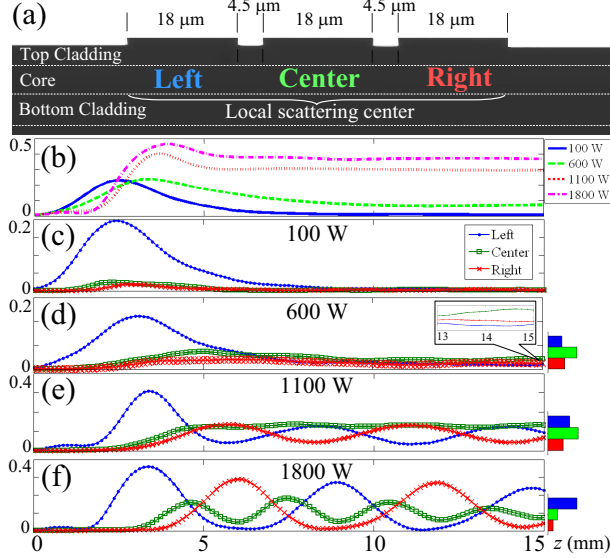


Fig. 2. (Color online) (a) An illustration of the sample's cross-section. (b)-(f) Propagation dynamics from numerical scattering simulations with  $\theta=6$  mrad; (b) fraction of the total power trapped within the entire GSC for various input powers in the range 100-1800 W; (c)-(f) fraction of the total power within each site for various input powers; (c) 100 W; (d) 600 W; (e) 1100 W; (f) 1800 W. Circles, left site; squares, central site; crosses, right site. Shown on the right are the output ( $z=15$  mm) energy distributions among the GSC sites

$\theta$ ) is used. A fraction of the incident light, having a larger effective propagation constant, can then couple to the linear modes of the local scatterers and trap there. In contrast with localized nonlinear waves, which are new bound states that form in *gaps* of a corresponding linear system (such as discrete [11,12], gap [13,14] and surface [15,16] solitons), here the nonlinear trapping (NLT) is into pre-existing linear modes of a local guiding scattering center (GSC). While switching of the NLT between the constituent sites of multi-site local GSCs has been demonstrated in silica glass as a function of  $\theta$  [10], *power dependent* switching has not been previously realized. This is due to the small strengths of available nonlinearities compared to the refractive index variations in previous experiments.

In this paper we report a realization of NLT switching, as a function of the input power, between adjacent sites in a specifically designed local GSC embedded in a nonlinear planar

AlGaAs waveguide. In the geometry considered here the Kerr nonlinearity is comparable to the spectral spacing between normal modes of different sites in the GSC, and the normal modes' propagation constants are close to the radiation modes' edge [see Figs. 1(c) and 1(d)]. A cross section of the sample is shown in Fig. 2(a). The cross section is constant along the propagation direction  $z$ , and the light was coupled to the  $1.5 \mu\text{m}$ -thick core layer, which was deposited on top of a  $1.5 \mu\text{m}$ -thick bottom cladding. While the homogeneous region surrounding the local scattering center has a top cladding layer of thickness  $0.22 \mu\text{m}$ , defining an effective refractive index of 3.32 in the transverse direction, in the GSC sites the top layer is  $1.5 \mu\text{m}$ -thick, defining an effective index which is larger than in the homogeneous region by 0.1%. Each of the three  $18 \mu\text{m}$ -wide sites then supports 3 normal modes. While directly excited local GSC modes are strongly-coupled to each other, they are decoupled from radiation modes in the linear regime.

Switching of the nonlinearly trapped power is first demonstrated in numerical simulations of the 1+1 nonlinear Schrödinger equation, using the beam propagation method [17]. The input beam is a  $20 \mu\text{m}$ -wide Gaussian beam, centered  $60 \mu\text{m}$  away from the center of the GSC and launched towards it at an angle of 6 mrad. Figure 2(b) shows propagation of the overall power in the GSC. For low input powers [solid line in Fig. 2(b)] the power leaks out of the GSC as it propagates along the  $z$  direction, and practically no power remains in the structure at the output position ( $z=15 \text{ mm}$ , corresponding to 3.1 diffraction lengths). This exponential decay of power within the GSC is characteristic of linear scattering. As the power is increased to nonlinear levels [dashed, dotted and dash-dotted lines in Fig. 2(b)] an increasing fraction of the power becomes trapped in the GSC region, due to NLT in the GSC's normal modes. Figs. 2(c)-2(f) show propagation of the power fraction within each site individually. At nonlinear powers, even though the overall trapped power remains constant indefinitely, it oscillates between the GSC sites with well determined amplitudes and phases, as evident by Figs. 2(e) and 2(f). By varying the beam intensity, the nonlinear coupling

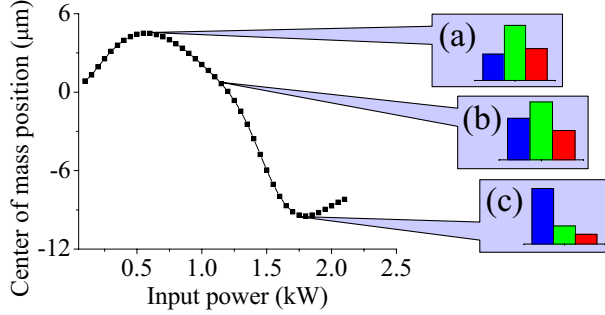


Fig. 3. (Color online) Position of the center of mass at the output ( $z=15$  mm) as a function of the input power, corresponding to the numerical simulations shown in Figs. 2(b)-2(f). Insets: output power distributions among the GSC sites at (a) 600 W; (a) 1100 W; (c) 1800 W.

between adjacent GSC sites is detuned, thus influencing the oscillations (both amplitude and phase) of the beam as it propagates through the GSC. The different oscillation amplitudes and slight phase shifts are eventually observed as different power distributions among the GSC sites at any output position. The alternation in the output power distribution can be conveniently described as a shift of its' center of mass. Figure 3 shows the output power's center of mass position as a function of the input power. The center of mass moves initially to the right [Fig. 3(a)] and then to the left [Figs. 3(b) and 3(c)]. Note that as the power is further increased the center of mass shifts back to the right, in agreement with the oscillatory nature of the trapped power dynamics.

To realize the NLT switching we have fabricated 15 mm-long nonlinear AlGaAs samples with a cross section as in Fig. 2(a). The excitation was by 100 fs laser pulses, at a 1 kHz repetition rate, generated by a Spectra Physics OPA, and yielding up to 10 kW peak power at a wavelength of 1520 nm. The input beam was shaped to a narrow 20  $\mu\text{m}$ -wide Gaussian at the input facet, and was coupled into the sample's homogeneous region. The beam was tilted at various angles  $\theta$  relative to the input facet towards the GSC. Variable neutral density filters were used to attenuate the input power, and a Vidicon camera was used to image the

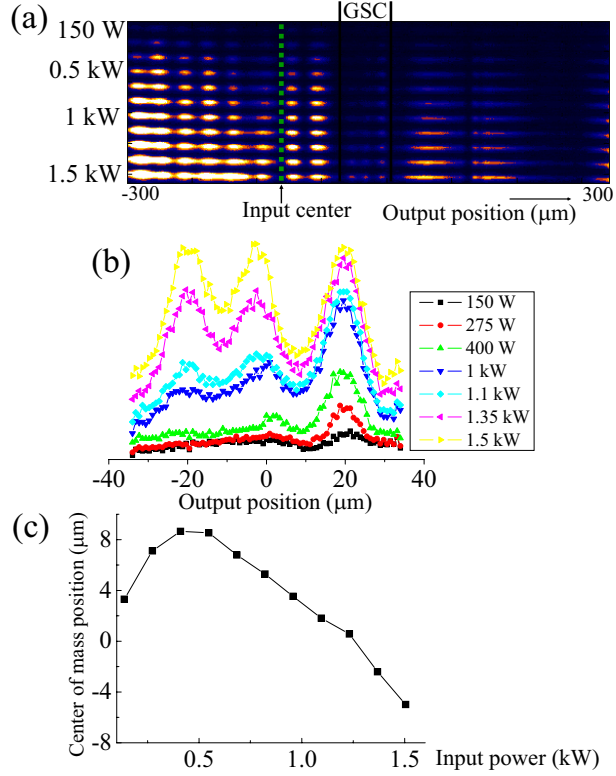


Fig. 4. (Color online) Experimental results with  $\theta=10$  mrad. (a) Output facet images at different input powers. (b) Power integrated along the vertical direction inside the GSC structure. (c) Power distribution's center of mass position as a function of the input power.

sample's output facet.

Experimental results for  $\theta=10$  mrad are presented in Fig. 4. The output facet images at different input powers [Fig. 4(a)], and the power distributions inside the structure, integrated along the vertical direction [Fig. 4(b)], clearly show a change in the output trapped power distribution as a function of the input power (while for low input powers only reflection and transmission wave packets are observed, in comparison to which the power inside the GSC is negligible). The corresponding output power's center of mass positions are shown in Fig. 4(c). The center of mass dynamics agree with the simulation results of Fig. 3, and demonstrate an initial shift of the center of mass towards the right site, in which most of the power is trapped, followed by a shift towards the central and left sites as the input power is

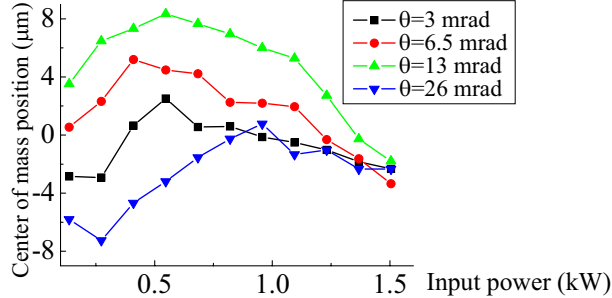


Fig. 5. (Color online) The output center of mass position as a function of the input power in experimental measurements with several excitation input angles.

further increased. The trapping and switching dynamics are extremely sensitive to the input angle  $\theta$ . Figure 5 shows the results of additional measurements, at different input angles, with all other parameters as in Fig. 4. It is evident from Figs. 4 and 5 that the extent of switching *at nonlinear power levels* (above 0.8 kW) changes as a function of the input angle, while it is suppressed altogether at some input angles (namely, below 5 mrad and above 20 mrad). In the latter case the trapping is static. However, there is a broad range of excitation angles (6-15 mrad) in which significant switching of the trapped power is observed.

In conclusion, we have demonstrated power dependent switching of the nonlinear trapping in 2D wave scattering by local multi-site guiding photonic potentials. Our experimental results prove that AlGaAs provides sufficient nonlinearity strengths for observable switching of the nonlinearly trapped power. This observation of NLT manipulation between GSCs, monolithically embedded in nonlinear planar waveguides, with the excitation power as a single parameter, can prove useful in optical switching applications. Our numerical simulations, which agree with the experimental results, also imply that tailored local potential profiles can lead to more prominent switching characteristics, which can be valuable in such applications.

This research was supported by the Israel Science Foundation through grant numbers 8006/03 and 944/05, and by NSERC in Canada.

## References

1. "Soliton-defect collisions in the nonlinear Schrodinger equation", X. D. Cao and B. A. Malomed, Phys. Lett. A **206**, 177 (1995).
2. "Resonant scattering of solitons", A. E. Miroshnichenko, S. Flach, and B. A. Malomed, Chaos **13**, 874 (2003).
3. "Resonant scattering of nonlinear Schrödinger solitons from potential wells", K. T. Stoychev, M. T. Primatarowa, and R. S. Kamburova, Phys. Rev. E **70**, 066622 (2004).
4. "Strong NLS soliton-defect interactions", R. H. Goodman, P. J. Holmes, and M. I. Weinstein, Physica D **192**, 215 (2004).
5. "Scattering of solitons and dark solitons by potential walls in the nonlinear schrodinger equation", H. Sakaguchi and M. Tamura, J. Phys. Soc. Jpn. **74**, 292 (2005).
6. "Scattering of topological solitons on holes and barriers", B. Piette, W. J. Zakrzewski, and J. Brand, J. Phys. A **38**, 10403 (2005).
7. "Transmission of matter-wave solitons through nonlinear traps and barriers", J. Garnier and F. Kh. Abdullaev, Phys. Rev. A **74**, 013604 (2006).
8. "Analytical study of resonant transport of Bose-Einstein condensates", K. Rapedius, D. Witthaut, and H. J. Korsch, Phys. Rev. A **73**, 033608 (2006).
9. "Enhanced quantum reflection of matter-wave solitons", C. Lee and J. Brand, Europhys. Lett. **73**, 321 (2006).
10. "Nonlinear scattering and trapping by local photonic potentials", Y. Linzon, R. Morandotti, M. Volatier, V. Aimez, R. Ares, and S. Bar-Ad, Phys. Rev. Lett. **99**, 133901 (2007).
11. "Discrete self-focusing in nonlinear arrays of coupled waveguides", D. N. Christodoulides and R. I. Joseph, Opt. Lett. **13**, 794 (1988).
12. "Discrete spatial optical solitons in waveguide arrays", H. S. Eisenberg, Y. Silberberg, R. Morandotti, A. R. Boyd, and J. S. Aitchison, Phys. Rev. Lett. **81**, 3383 (1998).

13. "Generation and stability of discrete gap solitons", A. A. Sukhorukov and Y. S. Kivshar, *Opt. Lett.* **28**, 2345 (2003).
14. "Gap solitons in waveguide arrays", D. Mandelik, R. Morandotti, J. S. Aitchison, and Y. Silberberg, *Phys. Rev. Lett.* **92**, 093904 (2004).
15. "Discrete surface solitons", K. G. Makris, S. Suntsov, D. N. Christodoulides, G. I. Stegeman, and A. Hache, *Opt. Lett.* **30**, 2466 (2005).
16. "Observation of discrete surface solitons", S. Suntsov, K. G. Makris, D. N. Christodoulides, G. I. Stegeman, A. Hache, R. Morandotti, H. Yang, G. Salamo, and M. Sorel, *Phys. Rev. Lett.* **96**, 063901 (2006).
17. R. W. Boyd, *Nonlinear Optics*, 2nd ed. (Academic Press, 2002).

## References

1. X. D. Cao and B. A. Malomed, *Phys. Lett. A* **206**, 177 (1995).
2. A. E. Miroshnichenko, S. Flach, and B. A. Malomed, *Chaos* **13**, 874 (2003).
3. K. T. Stoychev, M. T. Primatarowa, and R. S. Kamburova, *Phys. Rev. E* **70**, 066622 (2004).
4. R. H. Goodman, P. J. Holmes, and M. I. Weinstein, *Physica D* **192**, 215 (2004).
5. H. Sakaguchi and M. Tamura, *J. Phys. Soc. Jpn.* **74**, 292 (2005).
6. B. Piette, W. J. Zakrzewski, and J. Brand, *J. Phys. A* **38**, 10403 (2005).
7. J. Garnier and F. Kh. Abdullaev, *Phys. Rev. A* **74**, 013604 (2006).
8. K. Rapedius, D. Witthaut, and H. J. Korsch, *Phys. Rev. A* **73**, 033608 (2006).
9. C. Lee and J. Brand, *Europhys. Lett.* **73**, 321 (2006).
10. Y. Linzon, R. Morandotti, M. Volatier, V. Aimez, R. Ares, and S. Bar-Ad, *Phys. Rev. Lett.* **99**, 133901 (2007).
11. D. N. Christodoulides and R. I. Joseph, *Opt. Lett.* **13**, 794 (1988).

12. H. S. Eisenberg, Y. Silberberg, R. Morandotti, A. R. Boyd, and J. S. Aitchison, *Phys. Rev. Lett.* **81**, 3383 (1998).
13. A. A. Sukhorukov and Y. S. Kivshar, *Opt. Lett.* **28**, 2345 (2003).
14. D. Mandelik, R. Morandotti, J. S. Aitchison, and Y. Silberberg, *Phys. Rev. Lett.* **92**, 093904 (2004).
15. K. G. Makris, S. Suntsov, D. N. Christodoulides, G. I. Stegeman, and A. Hache, *Opt. Lett.* **30**, 2466 (2005).
16. S. Suntsov, K. G. Makris, D. N. Christodoulides, G. I. Stegeman, A. Hache, R. Morandotti, H. Yang, G. Salamo, and M. Sorel, *Phys. Rev. Lett.* **96**, 063901 (2006).
17. R. W. Boyd, *Nonlinear Optics*, 2nd ed. (Academic Press, 2002).